Near-Infrared Photoregulated Drug Release in Living Tumor Tissue via Yolk-Shell Upconversion Nanocages

Lingzhi Zhao, Juanjuan Peng, Qi Huang, Chunyan Li, Min Chen, Yun Sun, Qiuning Lin, Linyong Zhu, and Fuyou Li**

Phototrigger-controlled drug-release devices (PDDs) can be conveniently manipulated by light to obtain on-demand release patterns, thereby affording an improved therapeutic efficacy. However, no example of the PDDs has been demonstrated beyond the cellular level to date. By loading 7-amino-coumarin derivative caged anticancer drug chlorambucil to yolk–shell structured nanocages possessing upconversion nanophosphors (UCNPs) as moveable core and silica as mesoporous shell, a near-infrared (NIR)-regulated PDD is successfully created. In vitro experiments demonstrate that drug release from the PDD could be triggered by continuous-wave 980 nm light in a controlled pattern. The PDD could be taken up by cancer cells and release the drug to kill cancer cells upon NIR irradiation. Further in vivo studies demonstrate that the PDD can effectively response the NIR stimuli in living tissue. This is the first example of successful NIR-regulated drug release in living animal model. Such achievement resolves the problem of low tissue penetration depth for traditional PDDs by adopting UCNPs as an NIR light switcher, which gives impetus to practical applications.

1. Introduction

Phototrigger-controlled drug-release devices (PDDs) have emerged as promising tools for drug delivery as they can be conveniently manipulated by light to obtain on-demand release patterns, thereby affording better control of drug administration and improved therapeutic efficacy.[1] To date, several types of PDDs have been developed, including those based on scaffolds such as coumarin,[2] 2-nitrobenzyl,[3] and 7-nitroindoline.[4] However, traditional PDDs require UV light for excitation, which has poor penetration depth and is harmful to living tissues, thus limiting the practical application of PDDs in biomedicine.

Dr. L. Z. Zhao, J. J. Peng, Dr. C. Y. Li, M. Chen, Dr. Y. Sun, Prof. F. Y. Li
Department of Chemistry & The State Key Laboratory of Molecular Engineering of Polymers
Fudan University
Shanghai, 200433, P. R. China
E-mail: fyli@fudan.edu.cn
Q. Huang, Q. N. Lin, Prof. L. Y. Zhu
Shanghai Key Laboratory of Functional Materials Chemistry
East China University of Science and Technology
Shanghai, 200237, P.R. China
E-mail: linyongzhu@ecust.edu.cn

DOI: 10.1002/adfm.201302133

Near-infrared (NIR) light has received increasing popularity as an excitation source in biomedical applications due to their ability to penetrate deeply into tissues without causing harm.[5] NIR excitation has been employed in two-photon techniques using femtosecond pulsar lasers, which possess good focalization cross-section for nonlinear two-photon absorption.[6] However, not all photoresponsive molecules possess usable two-photon absorption efficiencies.[7] Even in materials with two-photon excitation capabilities, their low absorption cross-sections generally limit the rate and efficiency of the induced photoreactions.[8] By comparison, upconversion luminescence can be achieved through continuous-wave (CW) NIR excitation,[9] and thus represents an ideal technique for photochemical or imaging applications in vivo,[10,11] and in optical encoding or multiplexing of cells, biomolecules, and microspheres.[12] Lanthanide upconversion nanophosphors (UCNPs) co-doped with Yb^{3+} and Tm^{3+} are used to convert CW NIR light at 980 nm into UV emission in an anti-Stokes process.[9–11] Several groups have successfully developed phototriggers excited by UV upconversion emission for the photorelease of acetic acid[13] or dyes[14] as model molecules or for the photoactivation of macromolecules such as d-luciferin, DNA, or polymers.[15] Unfornately, although both upconversion and two-photon techniques possess deep tissue penetration ability with NIR excitation, no example of the photo-regulated drug release has been demonstrated beyond the cellular level to date. These reported upconversion- or two-photon systems for PDD are mainly limited to the low NIR-to-UV conversion efficiency.

We are interested in developing new UCNPs-based PDDs that drug-release inside the live animals could be remotely manipulated by NIR light. To fabricate an effective upconversion-based PDD, the system should show intense upconversion emission and high loading capacity to guarantee effective photo-uncaging of the enough drug to kill the cancer cells under upconversion excitation. In addition, effective photo-uncaging of the drug with zero premature release is needed.

In the present study, we demonstrate a new yolk-shell upconversion nanoparticle (YSUCNP, **Scheme 1**) which displayed intense NIR-to-UV emission and large pore volume and loaded with hydrophobized phototrigger-conjugated drug

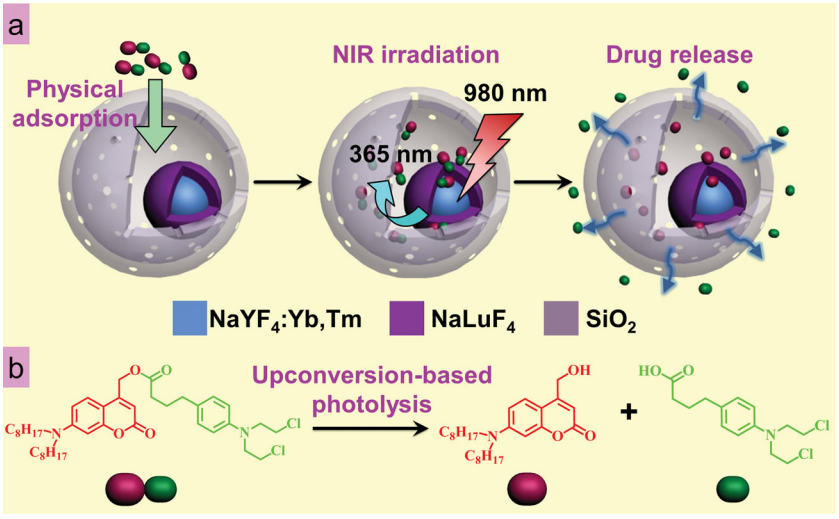

Scheme 1. Schematic illustration of the NIR-regulated upconversion-based PDD and the photolysis of the prodrug under upconversion emission from the YSUCNPs.

(amino-coumarin as phototrigger and chlorambucil as caged anticancer drug, denoted as ACCh) as a first example of upconversion-based PDDs worked in living tumor tissues. To prevent premature release, the phototrigger amino-coumarin was hydrophobized by two octyl groups. Some tests on tumor-bearing mice showed that the PDD can effectively respond to the CW-NIR excitation in living tissue, release the drug and thereby inhibit the growth rate of highly malignant sarcoma 180 (S180) tumors.

2. Results and Discussion

2.1. Design Strategy of the PDD

The yolk-shell nanoparticle which consists of a hybrid of core–shell and hollow structures,[16] is designed to achieve the following advantages. The hollow cavities can endow the material with a huge loading capacity for prodrug molecules for a sustainable release pattern.[17] Additionally, the mesoporous silica shell could avoid undesired premature release in living tissue by preventing contact between the adsorbed prodrug molecules and endogenous enzymes.[18] Consequently, the release of the drug can only be triggered by photolysis but not by enzymolysis. Moreover, to prevent the hosted prodrug from eluting from the cavity of the YSUCNPs under physiological conditions, the phototrigger amino-coumarin,[2b,2c] which photocages the anticancer drug chlorambucil, was specially hydrophobized. To obtain effective upconversion UV emission, a core–shell lanthanide nanocrystal was designed as the "yolk" center of the YSUCNPs. Herein, a heterogeneous core–shell nanocrystal ($NaYF_4$:Tm^{3+},Yb^{3+}@$NaLuF_4$) not homogeneous core–shell one ($NaLuF_4$:Tm^{3+},Yb^{3+}@$NaLuF_4$ or $NaYF_4$:Tm^{3+},Yb^{3+}@$NaYF_4$) is chosen, in order to charaterize the core–shell nanostructure easily by transmission electron microscopy (TEM) observation. Under excitation at CW 980 nm, the intense upconversion UV emission from the yolk center ($NaYF_4$:Tm^{3+},Yb^{3+}@$NaLuF_4$) can effectively drive the photolysis of the trigger ACCh to release the drug of chlorambucil (Scheme 1b), which diffuses out of the YSUCNPs through pores in the silica shell. At the same time, the degraded hydrophobic phototrigger molecules remain inside the YSUCNPs due to their high hydrophobicity (two octanyl chains), thus preventing the release of by-products into the surroundings.

2.2. Characterizations of the USNPs and YSUCNP

To achieve intense NIR-to-UV conversion of the nanosystem and charaterize the core–shell nanostructure easily by TEM analysis, heterogeneous core–shell particles with the core of the β-phase nanocrystal $NaYF_4$ co-doped with 30%Yb^{3+} and 0.5%Tm^{3+} ($NaYF_4$:Yb,Tm, see XRD patterns in Figure S1 in the Supporting Information) and the shell layer of pure $NaLuF_4$ were designed and synthesized through epitaxial growth[19] of $NaLuF_4$ shells onto $NaYF_4$:Yb,Tm cores (called as $NaYF_4$:Yb,Tm@$NaLuF_4$). The molar ratio of $NaYF_4$:Yb,Tm to $NaLuF_4$ in the core–shell nanoparticle was determined by inductively coupled plasma atomic emission spectrometer (ICP-AES) as 1:1.02, which is consist with the feed ratio in the synthesis procedure. **Figure 1**a,b displays the TEM images of $NaYF_4$:Yb,Tm (the core) and $NaYF_4$:Yb,Tm@$NaLuF_4$. An apparent enlargement of average nanoparticle size from 35 to 50 nm was observed after the coating process, indicating successful deposition of $NaLuF_4$ crystals onto the outer surface of $NaYF_4$:Yb,Tm. Furthermore, the core-shell structure of $NaYF_4$:Yb,Tm@$NaLuF_4$ containing different hosts in the core and shell layers was readily confirmed by element mapping of Lu and Y elements. As shown in Figure S2 in the Supporting Information, the distribution range of Y (red points) was encircled by the distribution range of Lu (green points), indicating the successful coating of the $NaLuF_4$ layer onto the nanocrystals.

Then, the upconversion properties of the $NaYF_4$:Yb,Tm@$NaLuF_4$ nanocrystals have been investigated. The upconversion emission at 345, 360, 450, 475, and 800 nm, corresponding to the $^3P_6 \rightarrow {}^3F_4$, $^1D_2 \rightarrow {}^3H_6$, $^1D_2 \rightarrow {}^3F_4$, $^1G_4 \rightarrow {}^3H_6$ and $^3H_4 \rightarrow {}^3H_6$ transitions,[9a] respectively, were observed for both $NaYF_4$:Yb,Tm and the core–shell $NaYF_4$:Yb,Tm@$NaLuF_4$ under excitation at CW 980 nm (**Figure 2**). However, the upconversion emission of the core–shell nanocrystals was significantly enhanced with ≈15 times compared to that of the $NaYF_4$ core alone. In particular, even if the upconversion emission at 800 nm ($^3H_4 \rightarrow {}^3H_6$ transition of Tm^{3+}) was normalized, the integral areas of upconversion emission in the 330–370 nm and 430–490 nm regions were increased by 6.1- and 4.1-fold, respectively. The enhancement of UV upconversion emission in the core-shell nanoparticles was anticipated to improve the response of the amino-coumarin phototrigger with maximum UV adsorption at 380 nm (Figure S3, Supporting Information) to the UV upconversion emission at 345 nm ($^3P_6 \rightarrow {}^3F_4$

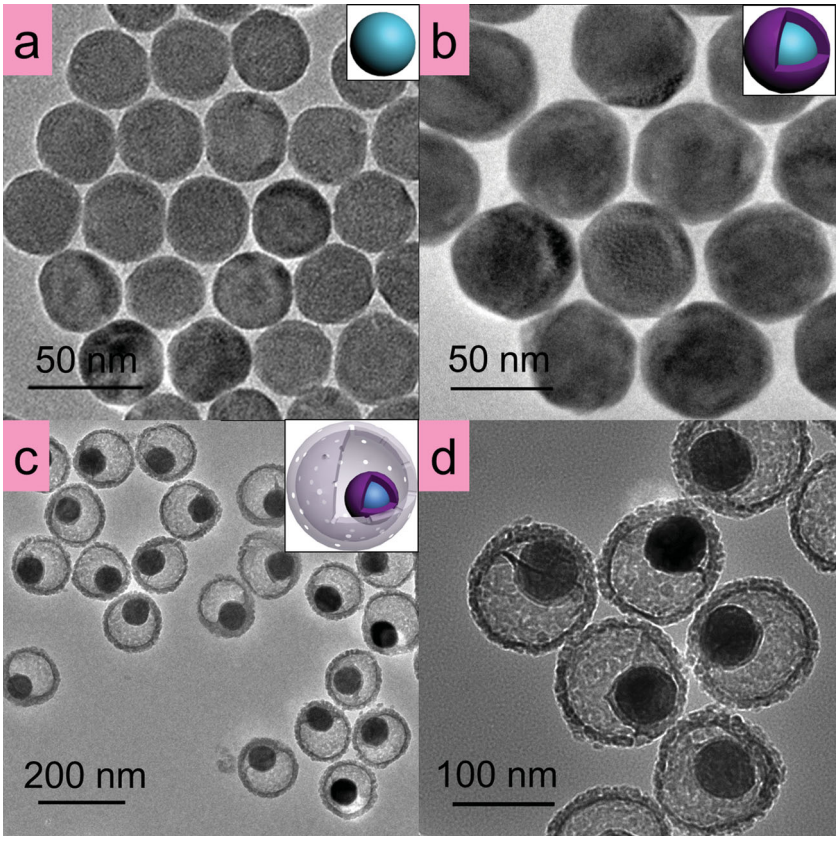

Figure 1. TEM images of the a) $NaYF_4$:Yb,Tm, b) $NaYF_4$:Yb,Tm@$NaLuF_4$, and c,d) YSUCNP nanoparticles.

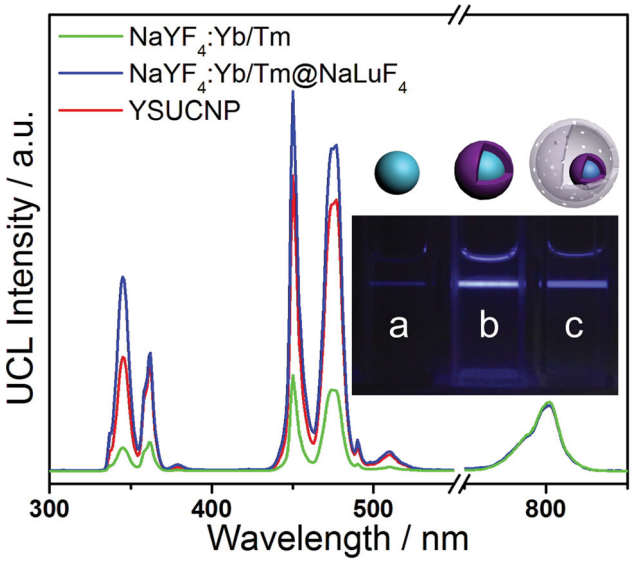

Figure 2. Upconversion emission spectra of the $NaYF_4$:Yb,Tm (green line), $NaYF_4$:Yb,Tm@$NaLuF_4$ (blue line) and YSUCNP (red line) nanoparticles under excitation at 980 nm. The upconversion emission intensities were normalized to the Tm emission at 800 nm ($^3H_4 \rightarrow {}^3H_6$). Inset: upconversion emission photos of the a) $NaYF_4$:Yb,Tm, b) $NaYF_4$:Yb,Tm@$NaLuF_4$, and c) YSUCNP nanoparticles in cyclohexane suspension with equal concentration of $NaYF_4$:Yb,Tm (1 mg mL^{-1}).

transition) and 360 nm ($^1D_2 \rightarrow {}^3H_6$ transition), respectively. Although the intensity of the UV emissions was only about half as the UCL in blue region ($^1D_2 \rightarrow {}^3F_4$ and $^1G_4 \rightarrow {}^3H_6$ transitions), the present UV light had already been effective enough to excite the phototrigger amino-coumarin, which was demonstrated in the in vitro drug release part.

Subsequently, a modified soft template[16a] method was employed to prepare the yolk-shell structured material with the $NaYF_4$:Yb,Tm@$NaLuF_4$ nanocrystals as the yolks and porous silica as the hollow shells. Herein, the yolk-shell structured upconversion nanoparticles were abbreviated as YSUCNPs. As shown in Figures 1c,d, rattle-like YSUCNPs were obtained, and each $NaYF_4$:Yb,Tm@$NaLuF_4$ yolk was encapsulated in a silica shell with a uniform thickness of 10 nm. Irregular mesopores on the silica shell can be observed from the high-resolution TEM image (Figure 1d), which allowed guest molecules to diffuse between the cavity and exterior environment. Furthermore, nitrogen adsorption-desorption analysis (**Figure 3**a) indicated that the YSUCNP possessed a relatively high pore volume of 0.96 $cm^3\ g^{-1}$ with a Brunauer–Emmett–Teller (BET) surface area of 195 $m^2\ g^{-1}$. Such a high pore volume is especially beneficial to increase the loading capacity of guest molecules.[17] The pore size distribution curve showed a narrow distribution peak at 1.7 nm with a 4.4 nm shoulder (Figure 3b), which confirmed the mesoporosity of the silica shell. Moreover, the YSUCNPs showed intense UV emission at 345 and 362 nm under CW excitation at 980 nm. The upconversion emission at 345 nm ($^3P_6 \rightarrow {}^3F_4$ transition) of the YSUCNPs with equal Tm^{3+} concentration decreased by 30% compared with the $NaYF_4$:Yb,Tm@$NaLuF_4$ yolk, but was still 4.3-fold higher than that of the $NaYF_4$:Yb,Tm nanoparticles, supporting the notion that the fabrication of the $NaYF_4$:Yb,Tm@$NaLuF_4$ core–shell structure was necessary for the activation of the phototrigger.

2.3. Drug Loading and Drug Release Assay in Solution

To prevent the prodrug and phototrigger from leaking into biological system, the phototrigger of amino-coumarin was specially hydrophobized with two octanyl chains and further conjugated with the anticancer drug chlorambucil to form the hydrophobic prodrug of amino-coumarin-caged chlorambucil (ACCh, Scheme 1b). The hydrophobic prodrug ACCh, which was dispersed in a solution of ethanol, was easily loaded inside the hollow inner cavity of YSUCNP by physical adsorption[20] through the mesopores on the shell. The prodrug-loaded sample is denoted as YSUCNP-ACCh. The loading ratio of ACCh was measured to be 710 μmol g^{-1} (49 wt%, 5.3×10^6 molecules per particle). Compared with the our previously

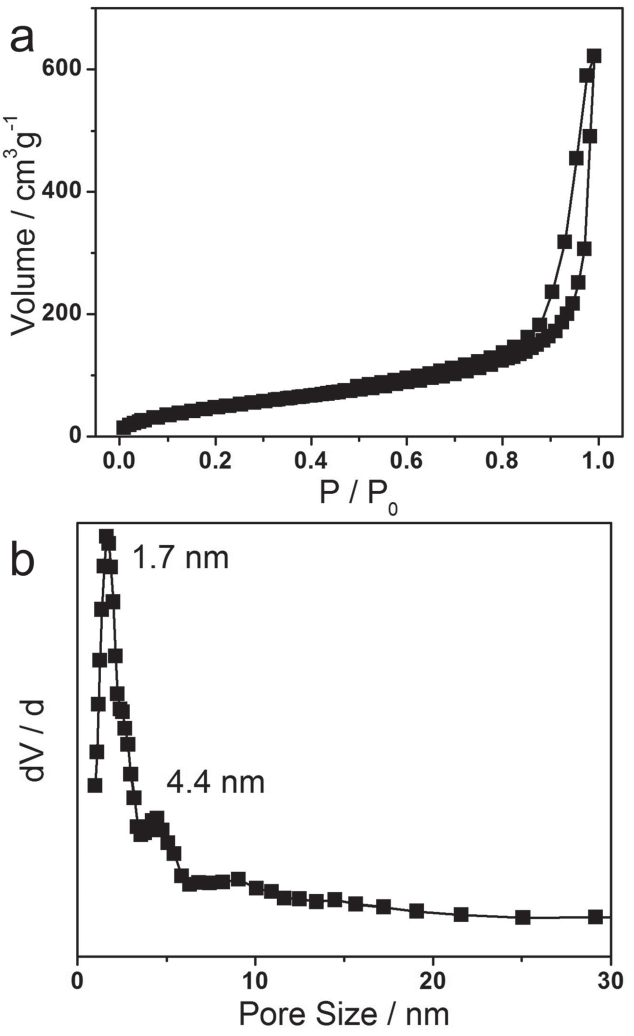

Figure 3. a) Nitrogen adsorption–desorption isotherms and b) Pore size distribution curve of YSUCNP. The pore size distribution is derived from the adsorption branches of the isotherms based on Barrett–Joyner–Halenda (BJH) model.

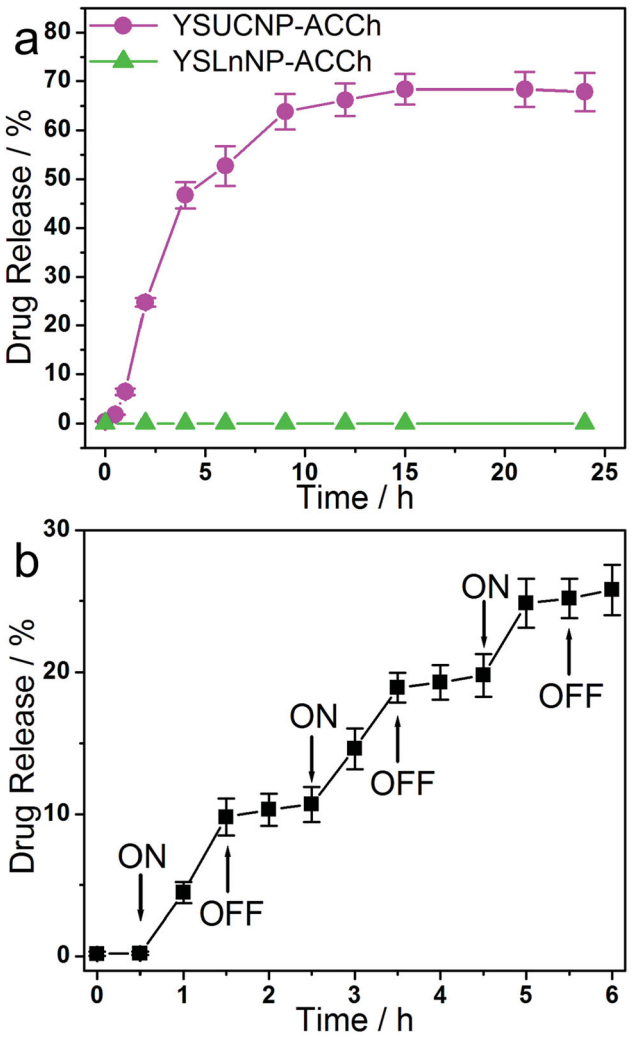

Figure 4. a) The release profiles of chlorambucil from YSUCNP-ACCh and YSLnNP-ACCh (control material) in PBS solution (pH = 7.5) under CW 980 nm irradiation, and b) the photo-regulated release of chlorambucil (drug) from YSUCNP-ACCh controlled by a 980 nm laser. "ON" and "OFF" indicate the initiation and termination of laser irradiation, respectively, and the working power density of the 980 nm laser was 570 mW cm^{-2}.

reported PDD using mesoporous silica nanoparticles as a host (103 μmol g^{-1})[7] and other upconversion-based photorelease systems (Table S1 in the Supporting Information), [13,15a,21] the loading efficiency of the YSUNCP system was dramatically increased. Such a high loading efficiency is beneficial for obtaining long-term controlled release of the encapsulated drug, as it can allow for longer drug release periods as well as less frequent drug administrations. The loaded prodrug was extremely stable in the nanocage even after soaking for 48 h in phosphate buffered saline (PBS) solution, as revealed by the lack of coumarin fluorescence in the surrounding solution, demonstrating no elution of ACCh from our designed PDD (data not shown).

NIR-regulated drug release from the YSUCNPs was performed in PBS solution. As shown in **Figure 4**a, irradiation of YSUCNPs with CW 980 nm light (570 mW cm^{-2}) effectively uncaged the chlorambucil from the coumarin derivative, resulting in >50% release of the drug chlorambucil within 6 hours, and a maximum release of about 68% of the drug after 15 h. In contrast, ≈80% of chlorambucil was released from YSUCNPs loaded with free chlorambucil after five hours (Figure S4, Supporting Information). The slower release rate of YSUCNP-ACCh could be ascribed to the relatively lower concentration of uncaged chlorambucil inside the hollow cavities. High performance liquid chromatography (HPLC) analysis revealed that no phototrigger amino-coumarin derivative escaped from YSUCNP into the suspension solution. These results confirmed that the chlorambucil could be uncaged by the upconversion process, while the hydrophobic amino-coumarin phototrigger was totally retained within the YSUCNP. The proportion of uncaged but unreleased chlorambucil retained inside the YSUCNP was determined to be 20% by HPLC analysis. These results indicated that the YSUCNP-ACCh functioned as an effective CW-NIR light-regulated PDD with a high photolysis efficiency of ≈88%. As a control, a similar yolk-shell nanoparticle consisting of the

$NaYF_4$:Yb@$NaLuF_4$ yolk without the Tm^{3+} activator (termed YSLnNP) was designed as a non-emissive material, which could also load ACCh with comparable capacity. However, upon 980 nm irradiation of ACCh-loaded YSLnNP (YSLnNP-ACCh, as control material) for 24 h, no uncaged chlorambucil was detected in the suspension of solution, which excluded the possibility of direct uncaging of chlorambucil by 980 nm light.

Moreover, the release of chlorambucil was clearly dependent on the on–off pattern of the excitation source (Figure 4b), indicating that the release dosage could be fine-tuned by remote control of the CW NIR irradiation under a power density of 570 mW cm^{-2}. The slight rise of drug concentration after the switching off of the excitation source could be attributed to the relatively slow mass transfer of chlorambucil from the YSUCNPs into the suspension solution, suggesting that the uncaging photolysis rate is greater than the drug diffusion rate. Compared with the nanoparticles enclosed with mesoporous silica and using a 420 nm laser as stimulus and acetonitrile/water (9:1 v/v) as release medium,[7] our NIR-controlled PDD showed a slower release rate in PBS in terms of percentage of drug released. As our nanostructures contain a larger loading ratio of drug, the release rates for the two types of PDDs are comparable (0.06 vs 0.08 μmol mL^{-1} in the first hour). More importantly, the higher loading capacity of YSUCNP gave rise to a sustainable release profile, especially at a lower working power density that was suitable for living tissue (50 mW cm^{-2}, Figure S5, Supporting Information). These properties favor the use of YSUNCPs in biomedicine because long-term release patterns can reduce drug administration frequency.[22]

Moreover, lipase enzymolysis was carried out to verify the stability of the YSUCNPs (**Figure 5**). Compared with ACCh suspension (release >60% chlorambucil within 8 h), only a small amount of released ACCh (3% within 48 h) was detected from YSUCNP-ACCh when incubated in the presence of 1.5 U mL^{-1} lipase in PBS. This result implies that the silica shell could successfully exclude lipase from the interior of the PDD.

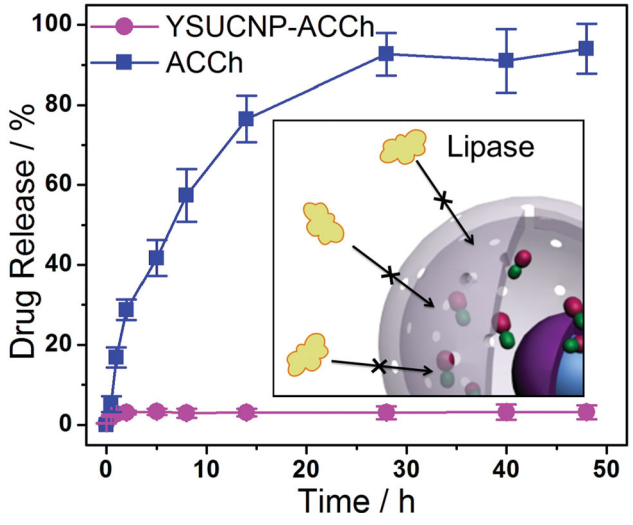

Figure 5. The lipase enzymolysis-induced chlorambucil release of ACCh suspension (control group) and YSUCNP-ACCh. Inset: the silica shell excludes lipase from the interior of the YSUCNP-ACCh system.

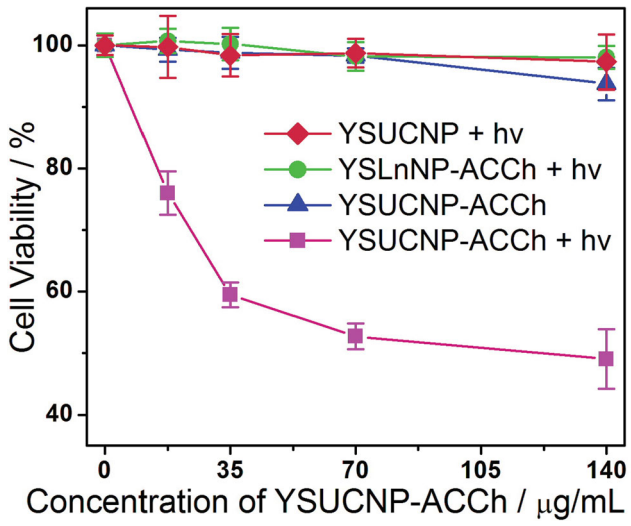

Figure 6. The viability of KB cells under different conditions. The concentration of YSUCNP-ACCh is 17.5, 35, 70, or 140 μg mL^{-1}, and the corresponding concentrations for YSUCNP + *hν* group is 8.8, 17.5, 35, or 70 μg mL^{-1}, respectively. *hν* stands for CW irradiation at 980 nm.

2.4. Evaluations of the NIR-Triggered PDD Using Cell and Animal Models

After incubation of KB cells with 5 mL, 70 μg mL^{-1} YSUCNP-ACCh, for six hours, a significant uptake of YSUCNP-ACCh into cells (6.4 pg per cell) could be detected, which was confirmed by confocal UCL cell imaging (Figure S6, Supporting Information). To demonstrate the effectiveness of the PDD, cell viability experiments were performed. As shown in **Figure 6**, after 30 min of 980 nm laser excitation (570 mW cm^{-2}), significant cell death was observed for the YSUCNP-ACCh + *hν* group, and the IC_{50} (half-maximal concentration of YSUCNP to cause cell death) was as low as ≈70 μg mL^{-1}, suggesting that the drug was uncaged and released into the cells, causing death. However, in other control groups (YSUCNP-ACCh, YSUCNP + *hν*, or YSLnNP-ACCh + *hν*), the viabilities of KB cells were all > 90%, confirming that NIR excitation, photo-cleavable drug, and UCNPs with UV upconversion emission capability were all indispensable elements for an effective NIR-excited PDD.

To realize NIR-regulated drug sustainable release in living tissue, drug administration experiments were carried out on tumor-bearing mice. A malignant murine tumor cell line S180 was selected as the tumor model. The PDD was intratumorally injected into tumor-bearing mice on the 1st day and on the 9th day, followed by exposure of 980-nm irradiation (50 mW cm^{-2}) for 20 min each day for 16 d. The low working power density is adopted to avoid undesired excessive heat effect generated by 980-nm laser. The tumor growth rate and mouse survival rate were monitored after the treatment with PDD. Compared to the control group (treated with saline), no significant difference in the normalized tumor volume was observed for the YSLnNP-ACCh group, which suggested neither the nanoparticle-encapsulated prodrug nor NIR radiation alone could affect tumor growth. Meanwhile, the YSUCNP-ACCh group showed a much slower tumor growth rate (**Figure 7**a). Typical photographs of

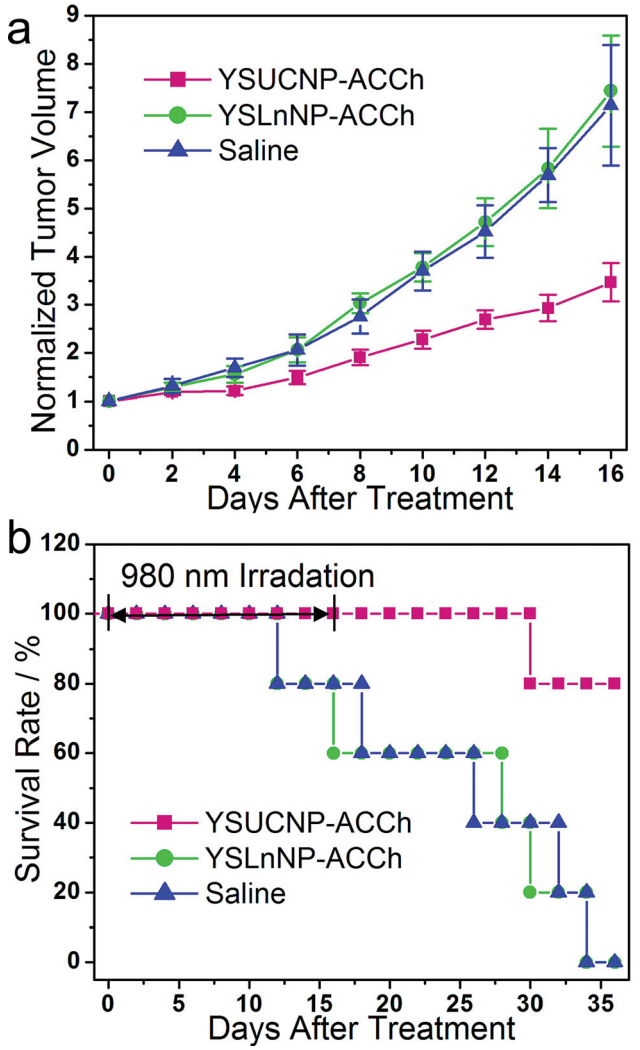

Figure 7. Photoregulated drug administration of YSUCNP-ACCh in living tumor tissue. a) The normalized S180 tumor volume and b) survival rate in mice intratumorally injected with 0.04 mL of 10 mg mL^{-1} YSUCNP-ACCh (purple line), YSLnNP-ACCh (green line) and 0.04 mL saline (blue line) on the 1st day and on the 9th day. In all mice groups, the tumors were exposed to 980 nm laser (50 mW cm^{-2}) for 20 min each day for 16 d.

mice from the YSUCNP-ACCh, YSLnNP-ACCh and silane groups are shown in **Figure 8**. In addition, the survival time of mice after YSUCNP-ACCh treatment was dramatically prolonged (Figure 7b). These results demonstrate that by adopting NIR light as an excitation source, the photoregulated drug-release of UCNPs-based PDD could be successfully realized in living organisms. The ineffective YSLnNP-ACCh treatment further confirmed that our PDD featured zero premature release even under actual physiological conditions, suggesting that the release of the drug could only be triggered by photolysis and not other hydrolytic events.

In vivo upconversion luminescence imaging revealed that the PDD with a drug loading ratio of 49 wt% remained at the injection site of the tumor tissue for at least one week after injection (Figure S7 in the Supporting Information). Thus, the PDD was administrated to the mice only twice with a long time interval of 7 d between injections. This administration frequency is much lower than that typically required for free drugs. Hence, the use of YSUCNP-ACCh can prolong the time interval between drug administrations, leading to reduced patient suffering.

In addition, toxicity assessment of YSUCNP was performed. Methyl thiazolyl tetrazolium (MTT) assay showed that there was only a slight decrease in the proliferation of KB cells incubated with YSUCNP (Figure S8 in the Supporting Information) in the range of 0–500 μg mL^{-1}, even after 24 h incubation with 500 μg mL^{-1} YSUCNP, cell viability was still maintained at >80%, revealing its low cytotoxicity of USUCNP. For histological study, no detectable lesion (e.g., necrosis, hydropic degeneration, inflammatory infiltrates, pulmonary fibrosis, gastroenteritis, or infectious diarrhea) was observed for mice intravenously injected with YSUCNP (Figure S9, Supporting Information). Serological assays were used to further evaluate the toxicity (Figure S10, Supporting Information), and also no significant fluctuations for the three most important hepatic function indicators total bilirubin (TBIL), alanine aminotransferase (ALT), and aspartate aminotransferase (AST) were obtained, as well as the enzyme levels and kidney functions urea (UREA) and creatinine (CRE). These results indicate the relative low toxicity of YSUCNP in the experiment condition.

3. Conclusions

We have demonstrated a yolk-shell structured, upconversion-based PDD with core–shell $NaYF_4$:Yb,Tm@$NaLuF_4$ nanocrystals as inner yolks. The anticancer drug chlorambucil, which was linked to the hydrophobized phototrigger of amino-coumarin derivative, could be loaded into the YSUCNP to produce YSUCNP-ACCh nanoparticles that show no premature release of drug under physiological conditions. Irradiation by a CW 980 nm laser triggers the upconversion cleavage of the amino-coumarin phototrigger, uncaging and releasing the drug chlorambucil from the YSUCNPs. Our innovative PDD possesses the advantages of high drug-loading capacity, zero premature release in living tissue and sensitivity to NIR light with deep tissue penetration depth. To our knowledge, this was the first successful demonstration of photoregulated drug release in living animal level. We envisage that our NIR-excited upconversion-based PDD could pave the way for the development of other photocontrolled drug delivery systems in the future and illuminate the bright prospects of the practical application of PDDs in biomedicine.

4. Experimental Section

Synthesis of $NaYF_4$:30%Yb,0.5%Tm Nanocrystals: The β-phase $NaYF_4$:Yb,Tm nanocrystals was synthesized via a solvothermal method.[23] YCl_3 (0.695 mmol), $YbCl_3$ (0.30 mmol), and $TmCl_3$ (0.005 mmol) were dispersed in oleic acid (OA, 8 mL) and octadecene (ODE, 15 mL), and then the mixture was heated to 160 °C for 30 min with a gentle flow of argon gas. After a homogeneous solution was formed, the mixture was cooled to room temperature, and followed by adding 8 mL methanol solution containing NaOH (2.5 mmol) and NH_4F (4 mmol). The temperature was heated to 60 °C to evaporate methanol, then was raised to 300 °C in an argon atmosphere for 60 min and

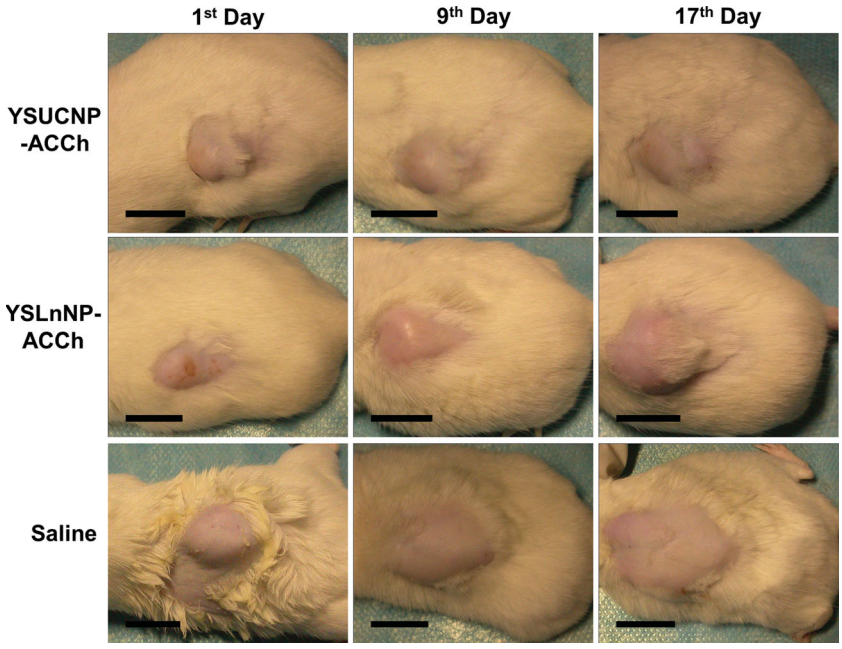

Figure 8. Representative photographs of tumor-bearing mice injected with YSUCNP-ACCh, YSLnNP-ACCh and saline on the 1st day, and after treatment on the 9th day and 17th day. Scale bars represent 1 cm.

cooled to room temperature naturally. The resulting nanoparticles were precipitated by adding ethanol, collected by centrifugation, and washed with cyclohexane/ethanol (1:1 v/v) for three times.

Synthesis of $NaYF_4$:Yb,Tm@$NaLuF_4$: The coating of the $NaLuF_4$ shell on the $NaYF_4$:Yb,Tm core was achieved through epitaxial growth via solvothermal method. 2 mL cyclohexane containing the as-prepared $NaYF_4$:Yb,Tm nanocrystals was mixed with $LuCl_3$ (1.0 mmol), OA (8 mL), and ODE (15 mL). The temperature was gently raised to 60 °C to remove cyclohexane. The following procedures were the same as the synthesis of $NaYF_4$:Yb,Tm nanoparticles.

Synthesis of YSUCNP: Before the synthesis, the OA ligand on the $NaYF_4$:Yb,Tm@$NaLuF_4$ surface was removed,[24] $NaYF_4$:Yb,Tm@$NaLuF_4$ (40 mg) was dispersed in aqueous solution (6 mL) and the pH was adjust to 2 by adding 0.5 m HCl solution. The obtained ligand-free $NaYF_4$:Yb,Tm@$NaLuF_4$ was recuperate by centrifugation, and redispersed in the mixed solution (20 mL) of surfactant lauryl sulfonatebetaine (LSB)/sodium dodecyl benzenesulfonate (SDBS) (5 mmol for each surfactant) to form a stock solution. The $NaYF_4$:Yb,Tm@$NaLuF_4$ stock solution (20 mL) was kept in a 40 °C oil bath for 30 min, then triethanolamine (50 µL), APS (47 µL), and TEOS (300 µL) were successively added to the resulting solution and stirred for another 1 h. The product was collected by centrifugation, washed with acetic acid/ethanol solution (1:19, v/v) for three times to remove the surfactant, and the obtained product YSUCNP was kept in ethanol for future applications.

Synthesis of ACCh: The synthetic routine of ACCh is shown in Scheme S1 in the Supporting Information. Compound 1 and 2 were synthesized according to literatures[25] with modifications (see Supporting Information).

Compound 3: SeO_2 (0.44 g, 4.0 mmol) and 2 (0.8 g, 2.0 mmol) were suspended in 50 mL p-xylene, the reaction mixture was refluxed under vigorous stirring with the protection of an argon atmosphere. After 48 h, the mixture was filtered and concentrated under reduced pressure. The dark brown residual oil was dissolved in methanol (50 mL), then sodium borohydride (0.15 g, 4.0 mmol) was added. The solution was stirred for 3 h at room temperature. Thereafter, the suspension was carefully neutralized with 1 mol L^{-1} HCl, diluted with H_2O, and partially concentrated under reduced pressure to remove methanol. The mixture was extracted with CH_2Cl_2 and the obtained organic phase was washed with H_2O and dried over Na_2SO_4, and concentrated in vacuum. The obtained oil was purified by column chromatography (*n*-hexane/EtOAc, 2:1, v/v) to yield 0.33 g (0.8 mmol, 40%) of 3 as a brown oil. ^{1}H NMR ($CDCl_3$, 400 MHz): δ = 7.34 (d, *J* = 8.8 Hz, 1H), 6.55 (dd, *J* = 8.8, 2 Hz, 1H), 6.46 (d, *J* = 2.8 Hz,1H), 6.26 (s, 1H),4.83 (s, 2H), 3.20 (t, *J* = 8 Hz, 4H), 1.56 (m, 4H), 1.28 (m, 20H), 0.88 (m, 6H); ^{13}C NMR ($CDCl_3$, 100MHz): 162.6, 156.1, 154.7, 150.8, 124.24, 108.7, 105.4, 97.9, 61.0, 51.3, 31.8, 29.4, 29.3, 27.1, 27.0, 22.6, 14.1; MS (EI): 416.3 [M+H].

Compound ACCh: Chlorambucil (180.0 mg, 0.6 mmol) was dissolved in 1.0 mL thionyl chloride at 0 °C and kept stirring for 3 h. Then the thionyl chloride was removed under vacuum to afford brown oil, which was kept in high vacuum for another 2 h. The obtained acid chloride was dissolved in dry CH_2Cl_2 (5 mL) for the esterification without further purification. In dark condition, to a solution of 3 (200.0 mg, 0.5 mmol), CH_2Cl_2 (10 mL) containing NEt_3 (130 µL, 0.9 mmol) was added above fresh prepared acid chloride. The mixture was stirred at room temperature for 24 h, and then the solvent was removed under reduced pressure. Purification with column chromatography (*n*-hexane/EtOAc, 5:1, v/v) gave 200.0 mg (0.3 mmol, 59% yield) of ACCh as brown soild. ^{1}H NMR($CDCl_3$, 400 MHz): δ = 7.27 (d, *J* = 8.8 Hz, 1H), 7.07 (d, *J* = 8.4 Hz, 2H), 6.64 (d, *J* = 8.4 Hz, 2H), 6.55 (dd, *J* = 9.2, 2.2 Hz, 1H), 6.49 (d, *J* = 2.4 Hz,1H), 6.12 (s, 1H), 5.20 (s, 2H), 3.69 (t, J = 6 Hz, 4H), 3.62 (t, *J* = 6 Hz, 4H), 3.3(t, *J* = 8 Hz, 4H), 2.59 (t, *J* = 7.6 Hz, 2H), 2.45 (t, *J* = 7.6 Hz, 2H), 1.97 (m, *J* = 7.6 Hz, 2H), 1.60 (m, 4H), 1.28 (m, 20H), 0.88 (m, 6H); ^{13}C NMR ($CDCl_3$, 100 MHz): 172.8, 162.0, 156.2, 149.55, 144.4, 130.3, 129.8, 124.2, 112.2, 108.9, 106.3, 98.1, 61.2, 53.6, 51.3, 40.5, 33.9, 33.4, 31.8, 29.4, 29.3, 27.1, 27.0, 26.6, 22.6, 14.1; HR-MS (EI): 701.3834 $[M+H]^+$.

Drug Loading: The prodrug ACCh (20 mg) was dissolved in ethanol (2 mL) and mixed with YSUCNP (10 mg). After being stirred at 35 °C for 72 h, the YSUCNP-ACCh was separated by centrifugation, gently washed with ethanol to remove the remaining unloaded ACCh, and dried at room temperature. The container of ACCh or ACCh solution in this experiment was tightly covered by tinfoil to avoid undesired photolysis.

NIR Phototrigger Controlled Drug Release of YSUCNP-ACCh in Solution: YSUCNP-ACCh was dispersed in pH = 7.5 PBS solution at an ACCh concentration of 1 mmol L^{-1} (1.4 mg mL^{-1} for YSUCNP-ACCh) and placed in a 5 mL cylindrical quartz tube with bottom area of ≈1 cm^2. The phototrigger controlled release was performed by irradiating the YSUCNP-ACCh suspension with CW 980 nm laser from the side of the tube (Scheme S2a, Supporting Information), and the working power densities were fixed at 570 mW cm^{-2} or 50 mW cm^{-2}. Small aliquot (100 µL) of the solution was withdraw at given time intervals and centrifuged at 10 000 r min^{-1} for 10 min. After irradiation for 24 h, the remaining YSUCNP-ACCh irradiated by NIR laser (570 mW cm^{-2}) was recovered by centrifugation, wash by methanol for three times, and the eluent was collected for further HPLC analysis. To obtain release profile of free chlorambucil, the drug was loaded in YSUCNP in a ratio of 710 µmol g^{-1}, and the chlorambucil-loaded YSUCNP was dispersed in PBS solution (pH = 7.5) at an ACCh concentration of 1 µmol mL^{-1}, the other experiment conditions including NIR irradiation were the same as the release of YSUCNP-ACCh. The cholrambucil concentration of the samples were analysed by an Aglient HPLC 1100 with a HC C-18 column (λ = 254 nm, 0.6 mL min^{-1} eluent: methanol-water 7/3 v/v).

Lipase Enzymolysis Experiment: YSUCNP-ACCh or ACCh powder was dispersed in 8 mL PBS solution (pH = 7.5) with 1% DMSO at an ACCh concentration of 1 µmol mL^{-1} (1.4 mg mL^{-1} for YSUCNP-ACCh),

kept in a 37 °C shaking table and stirred at 120 rpm for 0.5 h, then 4 mg porcine pancreas lipase was dissolved to the suspension to form 1.5 U mL^{-1} solution. Small aliquot (100 µL) of the solution was withdraw at given time intervals and centrifuged at 14 000 r min^{-1} for 10 min, the cholrambucil released by enzymolysis was analysed by HPLC as described above.

In Vitro Cell Viability Assay: KB cells were seeded in 96-well cell-culture plate at 1×10^4 per well and were incubated under 100% humidity at 37 °C, 5% CO_2 for 12 h, then different kinds of yolk-shell materials (YSUCNP, YSLnNP-ACCh and YSUCNP-ACCh, diluted in 100 µL RPMI 1640) at desired concentration were added to the wells of the treatment group. The cells were then incubated with the materials for 6 h to allow the endocytosis process. For the NIR irradiation experiment groups, the cell-culture plate was kept in a 25 °C water bath and exposed on CW 980 nm laser with a power density of 570 mW cm^{-2} from the top side of the plate (Scheme S2b, Supporting Information), the laser was turned off and on alternatively at a time interval of 5 min to prevent the cells from overheating by NIR light, until the accumulate irradiation time up to 30 min, and incubated for another 48 h at 37 °C under 5% CO_2. The cell viabilities were then measured by MTT method as described above.

To test the number of YSUCNP particles internalized by KB cells, 6×10^6 KB cells were seeded in a 10 cm Petri dish and were cultured as described above. The cells were incubated with 5 mL 140 µg mL^{-1} YSUCNP-ACCh suspension in RPMI 1640 for 6 h at 37 °C under 5% CO_2, followed by carefully washing cells with PBS solution. Then the cells were digested in a mixed solution of 0.25 mL HNO_3 (68%), 0.05 mL H_2O_2 (30%) for 2 d. The concentrations of Ln elements in the sample were determined by ICP-AES.

Photoregulated Drug Release in Living Tumor Tissue: Animal procedures were in agreement with the guidelines of the Institutional Animal Care and Use Committee. All animals were housed under standard environmental conditions, and acclimated for at least 24 h before experimentation. S-180 tumor mass were subcutaneously inoculated on the back of each male Kunming mouse (four weeks). The in vivo drug delivery treatment was carried out 24 d after tumor inoculation. YSLnNP-ACCh and YSUCNP-ACCh were dispersed in saline to from homogeneous suspensions (3.5 mmol mL^{-1} and 10 mg mL^{-1} for ACCh and YSUCNP-ACCh concerntrations, respectively). The 15 tumor-bearing Kunming mice were randomly divided into three groups, 0.04 mL of saline, YSLnNP-ACCh or YSUCNP-ACCh suspensions were intratumorally injected to each group. The phototriggered in vitro drug release was administrated by irradiate the tumors of every groups with a CW 980 nm laser (Shanghai Connet Fiber Optics Co., China) at a power density of 50 mW cm^{-2} for 20 min every day during the experiment (Scheme S2, Supporting Information). 0.04 mL of saline, YSLnNP-ACCh or YSUCNP-ACCh suspensions were injected to the corresponding group again at the 8^{th} day of irradiation, and the drug release administration was repeated for another 8 days. During the experiment, the length (l) and width (w) of the tumors were measured by a vernier caliper every other day, and the volume (V) of the tumor was calculated by the following formula: $V = 4\pi/3 \times lw^2$. For comparative purpose, the tumor volume was normalized by its initial volume as V/V_0 (V_0 was the volume of the tumor when the drug delivery was started).

For other experimental details, see the Supporting Information.

Supporting Information

Supporting Information is available from the Wiley Online Library or from the author.

Acknowledgements

This study was financially supported by NSFC (21231004), Shanghai Sci. Tech. Comm. (12JC1401300), MOST of China (2011AA03A407 and 2012CB932403), and the innovative team of Ministry of Education of China (IRT0911).

Received: June 23, 2013
Published online: September 4, 2013

[1] N. Fomina, J. Sankaranarayanan, A. Almutairi, *Adv. Drug Delivery Rev.* **2012**, *64*, 1005.
[2] a) N. K. Mal, M. Fujiwara, Y. Tanaka, *Nature* **2003**, *421*, 350; b) Q. N. Lin, C. Y. Bao, S. Y. Cheng, Y. L. Yang, W. Ji, L. Y. Zhu, *J. Am. Chem. Soc.* **2012**, *134*, 5052; c) Q. N. Lin, C. Y. Bao, Y. L. Yang, Q. N. Liang, D. S. Zhang, S. Y. Cheng, L. Y. Zhu, *Adv. Mater.* **2013**, *25*, 1981.
[3] P. Neveu, I. Aujard, C. Benbrahim, T. Le Saux, J. F. Allemand, S. Vriz, D. Bensimon, L. Jullien, *Angew. Chem. Int. Ed.* **2008**, *47*, 3744.
[4] G. Papageorgiou, D. C. Ogden, A. Barth, J. E. T. Corrie, *J. Am. Chem. Soc.* **1999**, *121*, 6503.
[5] a) L. Q. Xiong, Z. G. Chen, Q. W. Tian, T. Y. Cao, C. J. Xu, F. Y. Li, *Anal. Chem.* **2009**, *81*, 8687; b) Q. Liu, Y. Sun, T. S. Yang, W. Feng, C. G. Li, F. Y. Li, *J. Am. Chem. Soc.* **2011**, *133*, 17122; c) D. K. Chatteriee, A. J. Rufalhah, Y. Zhang, *Biomaterials* **2008**, *29*, 937.
[6] a) J. Babin, M. Pelletier, M. Lepage, J. F. Allard, D. Morris, Y. Zhao, *Angew. Chem. Int. Ed.* **2009**, *48*, 3329; b) S. Kumar, J. F. Allard, D. Morris, Y. L. Dory, M. Lepage, Y. Zhao, *J. Mater. Chem.* **2012**, *22*, 7252; c) S. Charier, A. Meglio, D. Alcor, E. Cogné-Laage, J.-F. Allemand, L. Jullien, A. Lemarchand, *J. Am. Chem. Soc.* **2005**, *127*, 15491.
[7] Q. N. Lin, Q. Huang, C. Y. Li, C. Y. Bao, Z. Z. Liu, F. Y. Li, L. Y. Zhu, *J. Am. Chem. Soc.* **2010**, *132*, 10645.
[8] W. Denk, *Proc. Natl. Acad. Sci. U. S. A.* **1994**, *91*, 6629.
[9] a) F. Auzel, *Chem. Rev.* **2004**, *104*, 139; b) F. Wang, X. G. Liu, *Chem. Soc. Rev.* **2009**, *38*, 976; c) C. X. Li, J. Lin, *J. Mater. Chem.* **2010**, *20*, 6831; d) M. Haase, H. Schafer, *Angew. Chem. Int. Ed.* **2011**, *50*, 5808; e) G. F. Wang, Q. Peng, Y. D. Li, *Acc. Chem. Res.* **2011**, *44*, 322; f) H. S. Mader, O. S. Wolfbeis, *Angew. Chem. Int. Ed.* **2013**, *52*, 2; g) J. Zhou, Z. Liu, F. Y. Li, *Chem. Soc. Rev.* **2012**, *41*, 1323; h) J. C. G. Bünzli, *Chem. Rev.* **2010**, *110*, 2729.
[10] a) L. Y. Wang, R. X. Yan, Z. Y. Hao, L. Wang, J. H. Zeng, H. Bao, X. Wang, Q. Peng, Y. D. Li, *Angew. Chem. Int. Ed.* **2005**, *44*, 6054; b) F. Wang, Y. Han, C. S. Lim, Y. H. Lu, J. Wang, J. Xu, H. Y. Chen, C. Zhang, M. H. Hong, X. G. Liu, *Nature* **2010**, *463*, 1061; c) J. N. Liu, W. B. Bu, L. M. Pan, S. Zhang, F. Chen, L. P. Zhou, K. L. Zhao, W. J. Peng, J. L. Shi, *Biomaterials* **2012**, *33*, 7282; d) F. Vetrone, R. Naccache, A. Zamarron, A. J. de la Fuente, F. Sanz-Rodriguez, L. M. Maestro, E. M. Rodriguez, D. Jaque, J. G. Sole, J. A. Capobianco, *ACS Nano* **2010**, *4*, 3254; e) F. Vetrone, R. Naccache, A. J. de la Fuente, F. Sanz-Rodriguez, A. Blazquez-Castro, E. M. Rodriguez, D. Jaque, J. G. Sole, J. A. Capobianco, *Nanoscale* **2010**, *2*, 495; f) D. M. Yang, G. G. Li, X. J. Kang, Z. Y. Cheng, P. A. Ma, C. Peng, H. Z. Lian, C. X. Li, J. Lin, *Nanoscale* **2012**, *4*, 3450; g) L. Cheng, K. Yang, Y. G. Li, J. H. Chen, C. Wang, M. W. Shao, S. T. Lee, Z. Liu, *Angew. Chem. Int. Ed.* **2011**, *50*, 7385; h) Q. Ju, D. T. Tu, Y. S. Liu, R. F. Li, H. M. Zhu, J. C. Chen, Z. Chen, M. D. Huang, X. Y. Chen, *J. Am. Chem. Soc.* **2012**, *134*, 1323; i) Y. S. Liu, S. Y. Zhou, D. T. Tu, Z. Chen, M. D. Huang, H. M. Zhu, E. Ma, X. Y. Chen, *J. Am. Chem. Soc.* **2012**, *134*, 15083; j) J. C. Zhou, Z. L. Yang, W. Dong, R. J. Tang, L. D. Sun, C. H. Yan, *Biomaterials* **2011**, *32*, 9059; k) X. F. Qiao, J. C. Zhou, J. W. Xiao, Y. F. Wang, L. D. Sun, C. H. Yan, *Nanoscale* **2012**, *4*, 4611.
[11] a) M. X. Yu, F. Y. Li, Z. G. Chen, H. Hu, C. Zhan, H. Yang, C. H. Huang, *Anal. Chem.* **2009**, *81*, 930; b) Q. Liu, Y. Sun, C. G. Li, J. Zhou, C. Y. Li, T. S. Yang, X. Z. Zhang, T. Yi, D. M. Wu, F. Y. Li,

ACS Nano **2011**, *5*, 3146; c) Q. Liu, T. S. Yang, W. Feng, F. Y. Li, *J. Am. Chem. Soc.* **2012**, *134*, 5390; d) L. M. Yao, J. Zhou, J. L. Liu, W. Feng, F. Y. Li, *Adv. Funct. Mater.* **2012**, *22*, 2667; f) Q. Liu, B. R. Yin, T. S. Yang, Y. C. Yang, Z. Shen, P. Yao, F. Y. Li, *J. Am. Chem. Soc.* **2013**, *135*, 5029.

[12] a) H. H. Gorris, R. Ali, S. M. Saleh, O. S. Wolfbeis, *Adv. Mater.* **2011**, *23*, 1652; b) H. H. Gorris, O. S. Wolfbeis, *Angew. Chem. Int. Edit.* **2013**, *52*, 3584; c) F. Zhang, Q. H. Shi, Y. C. Zhang, Y. F. Shi, K. L. Ding, D. Y. Zhao, G. D. Stucky, *Adv. Mater.* **2011**, *23*, 3775.

[13] C. J. Carling, F. Nourmohammadian, J. C. Boyer, N. R. Branda, *Angew. Chem. Int. Ed.* **2010**, *49*, 3782.

[14] a) B. Yan, J. C. Boyer, N. R. Branda, Y. Zhao, *J. Am. Chem. Soc.* **2011**, *133*, 19714; b) B. Yan, J. C. Boyer, D. Habault, N. R. Branda, Y. Zhao, *J. Am. Chem. Soc.* **2012**, *134*, 16558.

[15] a) Y. M. Yang, Q. Shao, R. R. Deng, C. Wang, X. Teng, K. Cheng, Z. Cheng, L. Huang, Z. Liu, X. G. Liu, B. G. Xing, *Angew. Chem. Int. Ed.* **2012**, *51*, 3125; b) Y. M. Yang, B. Velmurugan, X. G. Liu, B. G. Xing, *Small* **2013**, DOI: 10.1002/smll.201201765; c) M. K. G. Jayakumar, N. M. Idris, Y. Zhang, *Proc. Natl. Acad. Sci. U. S. A.* **2012**, *109*, 8483; d) Y. M. Yang, F. Liu, X. G. Liu, B. G. Xing, *Nanoscale* **2013**, *5*, 231.

[16] a) X. J. Wu, D. S. Xu, *J. Am. Chem. Soc.* **2009**, *131*, 2774; b) J. Liu, S. Z. Qiao, S. B. Hartono, G. Q. Lu, *Angew. Chem. Int. Ed.* **2010**, *49*, 4981; c) K. Kamata, Y. Lu, Y. N. Xia, *J. Am. Chem. Soc.* **2003**, *125*, 2384; d) Y. D. Yin, R. M. Rioux, C. K. Erdonmez, S. Hughes, G. A. Somorjai, A. P. Alivisatos, *Science* **2004**, *304*, 711.

[17] Y. F. Zhu, J. L. Shi, W. H. Shen, X. P. Dong, J. W. Feng, M. L. Ruan, Y. S. Li, *Angew. Chem. Int. Ed.* **2005**, *44*, 5083.

[18] a) Y. J. Wang, F. Caruso, *Chem. Commun.* **2004**, 1528; b) A. R. Zimmerman, J. Chorover, K. W. Goyne, S. L. Brantley, *Environ. Sci. Technol.* **2004**, *38*, 4542.

[19] F. Wang, R. R. Deng, J. Wang, Q. X. Wang, Y. Han, H. M. Zhu, X. Y. Chen, X. G. Liu, *Nat. Mater.* **2011**, *10*, 968.

[20] a) J. Lu, M. Liong, J. I. Zink, F. Tamanoi, *Small* **2007**, *3*, 1341; b) C. Kim, S. Kim, W. K. Oh, M. Choi, J. Jang, *Chem. Eur. J.* **2012**, *18*, 4902.

[21] a) C. Wang, L. A. Cheng, Z. Liu, *Biomaterials* **2011**, *32*, 1110; b) G. Tian, Z. J. Gu, L. J. Zhou, W. Y. Yin, X. X. Liu, L. Yan, S. Jin, W. L. Ren, G. M. Xing, S. J. Li, Y. L. Zhao, *Adv. Mater.* **2012**, *24*, 1226; c) J. N. Liu, W. B. Bu, L. M. Pan, J. L. Shi, *Angew. Chem. Int. Edit.* **2013**, *52*, 4375.

[22] W. Aughenbaugh, S. Radin, P. Ducheyne, *J. Biomed. Mater. Res.* **2001**, *57*, 321.

[23] Z. Q. Li, Y. Zhang, *Nanotechnology* **2008**, *19*, 345606.

[24] N. Bogdan, F. Vetrone, G. A. Ozin, J. A. Capobianco, *Nano Lett.* **2011**, *11*, 835.

[25] a) J. Wojtyk, A. McKerrow, P. Kazmaier, E. Buncel, *Can. J. Chem.* **1999**, *77*, 903; b) S. Y. Park, Y. Kubota, K. Funabiki, M. Matsui, *Chem. Lett.* **2009**, *38*, 162.